An SVD in Spherical Surface Wave Tomography

Ralf Hielscher, Daniel Potts and Michael Quellmalz

Abstract In spherical surface wave tomography, one measures the integrals of a function defined on the sphere along great circle arcs. This forms a generalization of the Funk–Radon transform, which assigns to a function its integrals along full great circles. We show a singular value decomposition (SVD) for the surface wave tomography provided we have full data.

Since the inversion problem is overdetermined, we consider some special cases in which we only know the integrals along certain arcs. For the case of great circle arcs with fixed opening angle, we also obtain an SVD that implies the injectivity, generalizing a previous result for half circles in [Groemer, On a spherical integral transform and sections of star bodies, Monatsh. Math., 126(2):117–124, 1998]. Furthermore, we derive a numerical algorithm based on the SVD and illustrate its merchantability by numerical tests.

1 Introduction

While the famous two-dimensional Radon transform assigns to a function $f\colon \mathbb{R}^2 \to \mathbb{R}$ all its line integrals, its spherical generalization, the Funk–Radon transform $\mathscr{F}\colon C(\mathbb{S}^2) \to C(\mathbb{S}^2)$, assigns to a function on the two-dimensional sphere $\mathbb{S}^2 = \{\boldsymbol{\xi} \in \mathbb{R}^3 : |\boldsymbol{\xi}| = 1\}$ its integrals

----

Ralf Hielscher

Chemnitz University of Technology, Faculty of Mathematics, Reichenhainer Straße 39, 09126 Chemnitz, Germany, e-mail: `ralf.hielscher@mathematik.tu-chemnitz.de`

Daniel Potts
Same department, e-mail: `daniel.potts@mathematik.tu-chemnitz.de`

Michael Quellmalz
Same department, e-mail: `michael.quellmalz@mathematik.tu-chemnitz.de`

$$\mathscr{F}f(\boldsymbol{\xi}) = \frac{1}{2\pi} \int_{\langle \boldsymbol{\xi}, \boldsymbol{\eta} \rangle = 0} f(\boldsymbol{\eta}) \, \mathrm{d}\boldsymbol{\eta}, \qquad \boldsymbol{\xi} \in \mathbb{S}^2,$$

along all great circles $\{\boldsymbol{\eta} \in \mathbb{S}^2 : \boldsymbol{\eta} \perp \boldsymbol{\xi}\}$, $\boldsymbol{\xi} \in \mathbb{S}^2$. The investigation of the Funk–Radon transform dates back to the work of Funk [11], who showed the injectivity of the operator $\mathscr{F}$ for even functions. In other publications, the operator $\mathscr{F}$ is also known as Funk transform, Minkowski–Funk transform or spherical Radon transform.

Similar to the Radon transform, the Funk–Radon transform plays an important role in imaging. Motivated by specific imaging modalities, the Funk–Radon transform has been generalized further to other paths of integration, namely circles with fixed diameter [38, 34], circles containing the north pole [1, 5, 20, 35], circles perpendicular to the equator [12, 44, 23], and nongeodesic hyperplane sections of the sphere [37, 33, 30, 31]. The integrals along half great circles have been investigated in [18, 13, 36]. Interestingly, some of these generalizations lead to injective operators.

In this paper, we replace the great circles as paths of integration in the Funk–Radon transform by great circle arcs with arbitrary opening angle. Let $\boldsymbol{\xi}, \boldsymbol{\zeta} \in \mathbb{S}^2$ be two points on the sphere that are not antipodal and denote by $\gamma(\boldsymbol{\xi}, \boldsymbol{\zeta})$ the shortest geodesic connecting both points. Then we aim at recovering $f \colon \mathbb{S}^2 \to \mathbb{C}$ from the integrals

$$g(\boldsymbol{\xi}, \boldsymbol{\zeta}) = \int_{\gamma(\boldsymbol{\xi}, \boldsymbol{\zeta})} f(\boldsymbol{\eta}) \, \mathrm{d}\boldsymbol{\eta}, \quad \boldsymbol{\xi}, \boldsymbol{\zeta} \in \mathbb{S}^2, \boldsymbol{\xi} \neq -\boldsymbol{\zeta}. \tag{1}$$

The study of this problem is motivated by spherical surface wave tomography. There, one measures the time a seismic wave travels along the Earth's surface from an epicenter to a receiver. Knowing the traveltimes of such waves between many pairs of epicenters and receivers, one wants to recover the local phase velocity. A common approach is the great circle ray approximation, where it is assumed that a wave travels along the arc of the great circle connecting epicenter and receiver. Then the traveltime of the wave equals the integral of the "slowness function" along the great circle arc connecting the epicenter and the receiver, where the slowness function is defined as one over the local phase velocity [43, 40, 29]. Hence, recovering the local phase velocity as a real-valued spherical function from its mean values along certain arcs of great circles is modeled by (1), see [3].

Although (1) uses a very intuitive parametrization of great circle arcs on the sphere, it is not well suited for analyzing the underlying operator since the arc length is restricted to $[0, \pi)$ and, even for continuous f, the function g has no continuous extension to a function on $\mathbb{S}^2 \times \mathbb{S}^2$. Therefore, we parameterize the manifold of all great circle arcs by the arclength $2\psi \in [0, 2\pi]$ and the rotation $Q \in \mathrm{SO}(3)$ that maps the arc of integration to the equator such that the midpoint of the arc is mapped to $(1, 0, 0)^\top$. Using this parametrization, the arc transform is defined in Section 3.1 as an operator

$$\mathscr{A} \colon C(\mathbb{S}^2) \to C(\mathrm{SO}(3) \times [0, \pi]).$$

In Theorem 3.3, we derive a singular value decomposition of $\mathscr{A}$, which involves spherical harmonics in $L^2(\mathbb{S}^2)$ and Wigner-D functions in $L^2(\mathrm{SO}(3) \times [0, \pi])$. Furthermore, we give upper and lower bounds for the singular values.

Since the function f lives on a two-dimensional manifold but the transformed function $\mathscr{A}f$ lives on a four-dimensional manifold, the inverse problem is highly overdetermined. For this reason, we consider in Section 4 specific subsets of arcs that still allow for the reconstruction of the function f. Most notably, we investigate in Section 4.3 the restriction of the arc transform to arcs of constant opening angle. This restriction includes as special cases the ordinary Funk–Radon transform as well as the half circle transform [18]. For the restricted operator, we prove in Theorem 4.4 a singular value decomposition and show that the singular values decay as $(n + \frac{1}{2})^{-\frac{1}{2}} C(\psi, n)$. While for opening angles $2\psi < \pi$ the constant $C(\psi, n)$ is independent of n, it converges to zero for odd n and $2\psi \to 2\pi$.

Finally, we present in Section 5 a numerical algorithm for the arc transform with fixed opening angle, which is based on the nonequispaced fast spherical Fourier transform [25] and the nonequispaced fast $\mathrm{SO}(3)$ Fourier transform [32].

2 Fourier analysis on $\mathbb{S}^2$ and $\mathrm{SO}(3)$

In this section, we present some basic facts about harmonic analysis on the sphere $\mathbb{S}^2$ and the rotation group $\mathrm{SO}(3)$ and introduce the notation we will use later on.

2.1 Harmonic analysis on the sphere

In this section, we are going to summarize some basic facts about harmonic analysis on the sphere as it can be found, e.g., in [28, 7, 10]. We denote by $\mathbb{Z}$ the set of integers and with $\mathbb{N}_0$ the nonnegative integers.

We define the two-dimensional sphere $\mathbb{S}^2 = \{\boldsymbol{\xi} \in \mathbb{R}^3 : |\boldsymbol{\xi}| = 1\}$ as the set of unit vectors $\boldsymbol{\xi} = (\xi_1, \xi_2, \xi_3)^\top$ in the three-dimensional Euclidean space and make use of its parametrization in terms of the spherical coordinates

$$\boldsymbol{\xi}(\varphi, \vartheta) = (\cos\varphi \sin\vartheta, \sin\varphi \sin\vartheta, \cos\vartheta)^\top, \quad \varphi \in [0, 2\pi), \ \vartheta \in [0, \pi].$$

Let $f \colon \mathbb{S}^2 \to \mathbb{C}$ be some measurable function. With respect to spherical coordinates, the surface measure $\mathrm{d}\boldsymbol{\xi}$ on the sphere reads as

$$\int_{\mathbb{S}^2} f(\boldsymbol{\xi}) \, \mathrm{d}\boldsymbol{\xi} = \int_0^\pi \int_0^{2\pi} f(\boldsymbol{\xi}(\varphi, \vartheta)) \sin\vartheta \, \mathrm{d}\varphi \, \mathrm{d}\vartheta.$$

The Hilbert space $L^2(\mathbb{S}^2)$ is the space of all measurable functions $f \colon \mathbb{S}^2 \to \mathbb{C}$ whose norm $\|f\|_{L^2(\mathbb{S}^2)} = (\langle f,f \rangle_{L^2(\mathbb{S}^2)})^{1/2}$ is finite, where $\langle f,g \rangle_{L^2(\mathbb{S}^2)} = \int_{\mathbb{S}^2} f(\boldsymbol{\xi}) \overline{g(\boldsymbol{\xi})}\, \mathrm{d}\boldsymbol{\xi}$ denotes the usual L^2–inner product.

We define the associated Legendre functions

$$P_n^k(t) = \frac{(-1)^k}{2^n n!} \left(1 - t^2\right)^{k/2} \frac{\mathrm{d}^{n+k}}{\mathrm{d}t^{n+k}} \left(t^2 - 1\right)^n, \quad t \in [-1,1],$$

of degree $n \in \mathbb{N}_0$ and order $k = 0,\dots,n$. We define the normalized associated Legendre functions by

$$\widetilde{P}_n^k = \sqrt{\frac{2n+1}{4\pi} \frac{(n-k)!}{(n+k)!}}\, P_n^k \tag{2}$$

and

$$\widetilde{P}_n^{-k} = (-1)^k\, \widetilde{P}_n^k,$$

where the factor $(-1)^k$ is called Condon–Shortley phase, which is omitted by some authors.

An orthonormal basis in the Hilbert space $L^2(\mathbb{S}^2)$ of square integrable functions on the sphere is formed by the spherical harmonics

$$Y_n^k(\boldsymbol{\xi}(\varphi,\vartheta)) = \widetilde{P}_n^k(\cos\vartheta)\, \mathrm{e}^{\mathrm{i}k\varphi} \tag{3}$$

of degree $n \in \mathbb{N}_0$ and order $k = -n,\dots,n$. Accordingly, any function $f \in L^2(\mathbb{S}^2)$ can be expressed by its spherical Fourier series

$$f = \sum_{n=0}^{\infty} \sum_{k=-n}^{n} \hat{f}_n^k Y_n^k$$

with the spherical Fourier coefficients

$$\hat{f}_n^k = \int_{\mathbb{S}^2} f(\boldsymbol{\xi})\, \overline{Y_n^k(\boldsymbol{\xi})}\, \mathrm{d}\boldsymbol{\xi}, \quad n \in \mathbb{N}_0,\ k = -n,\dots,n.$$

We define the space of spherical polynomials of degree up to $N \in \mathbb{N}_0$ by

$$\mathscr{P}_N = \mathrm{span}\left\{Y_n^k : n = 0,\dots,N,\ k = -n,\dots,n\right\}.$$

2.2 Rotational harmonics

We state some facts about functions on the rotation group $\mathrm{SO}(3)$. This introduction is based on [19], rotational Fourier transforms date back to Wigner, 1931, see [42]. The rotation group $\mathrm{SO}(3)$ consists of all orthogonal 3×3–matrices with determinant one equipped with the matrix multiplication as group operation. Every rotation $Q \in \mathrm{SO}(3)$ can be expressed in terms of its Euler angles α,β,γ by

$$Q(\alpha, \beta, \gamma) = R_3(\alpha) R_2(\beta) R_3(\gamma), \quad \alpha, \gamma \in [0, 2\pi), \ \beta \in [0, \pi],$$

where $R_i(\alpha)$ denotes the rotation of the angle α about the $\boldsymbol{\xi}_i$–axis, i.e.,

$$R_3(\alpha) = \begin{pmatrix} \cos\alpha & -\sin\alpha & 0 \\ \sin\alpha & \cos\alpha & 0 \\ 0 & 0 & 1 \end{pmatrix}, \qquad R_2(\beta) = \begin{pmatrix} \cos\beta & 0 & \sin\beta \\ 0 & 1 & 0 \\ -\sin\beta & 0 & \cos\beta \end{pmatrix}.$$

Note that we use this *zyz*-convention of Euler angles throughout this paper. The integral of a function $g \colon \mathrm{SO}(3) \to \mathbb{C}$ on the rotation group is given by

$$\int_{\mathrm{SO}(3)} g(Q)\,\mathrm{d}Q = \int_0^{2\pi} \int_0^\pi \int_0^{2\pi} g(Q(\alpha, \beta, \gamma)) \sin(\beta)\,\mathrm{d}\alpha\,\mathrm{d}\beta\,\mathrm{d}\gamma.$$

We define the rotational harmonics or Wigner D-functions $D_n^{k,j}$ of degree $n \in \mathbb{N}_0$ and orders $k, j \in \{-n, \ldots, n\}$ by

$$D_n^{k,j}(Q(\alpha, \beta, \gamma)) = \mathrm{e}^{-\mathrm{i}k\alpha} d_n^{k,j}(\cos\beta) \mathrm{e}^{-\mathrm{i}j\gamma},$$

where the Wigner d-functions are given by [41, p. 77]

$$d_n^{k,j}(t) = \frac{(-1)^{n-j}}{2^n} \sqrt{\frac{(n+k)!(1-t)^{j-k}}{(n-j)!(n+j)!(n-k)!(1+t)^{j+k}}} \left(\frac{\mathrm{d}}{\mathrm{d}t}\right)^{n-k} \frac{(1+t)^{n+j}}{(1-t)^{-n+j}}.$$

The Wigner d-functions satisfy the orthogonality relation

$$\int_{-1}^1 d_n^{k,j}(t)\, d_{n'}^{k,j}(t)\,\mathrm{d}t = \frac{2\delta_{n,n'}}{2n+1}.$$

We define the space of square-integrable functions $L^2(\mathrm{SO}(3))$ with inner product $\langle f, g \rangle_{L^2(\mathrm{SO}(3))} = \int_{\mathrm{SO}(3)} f(Q)\overline{g(Q)}\,\mathrm{d}Q$. By the Peter–Weyl theorem, the rotational harmonics $D_n^{k,j}$ are complete in $L^2(\mathrm{SO}(3))$ and satisfy the orthogonality relation

$$\left\langle D_n^{k,j}, D_{n'}^{k',j'} \right\rangle_{L^2(\mathrm{SO}(3))} = \int_{\mathrm{SO}(3)} D_n^{k,j}(Q)\, \overline{D_{n'}^{k',j'}(Q)}\,\mathrm{d}Q = \frac{8\pi^2}{2n+1}\,\delta_{n,n'}\delta_{k,k'}\delta_{j,j'}. \quad (4)$$

We define the rotational Fourier coefficients of $g \in L^2(\mathrm{SO}(3))$ by

$$\hat{g}_n^{k,j} = \frac{2n+1}{8\pi^2} \left\langle g, D_n^{k,j} \right\rangle_{L^2(\mathrm{SO}(3))}, \quad n \in \mathbb{N}_0,\ k, j = -n, \ldots, n. \quad (5)$$

Then the rotational Fourier expansion of g holds

$$g = \sum_{n=0}^\infty \sum_{k,j=-n}^n \hat{g}_n^{k,j} D_n^{k,j}.$$

The rotational Fourier transform is also known as $SO(3)$ Fourier transform (SOFT) or Wigner D-transform.

The rotational harmonics $D_n^{k,j}$ are eigenfunctions of the Laplace–Beltrami operator on $SO(3)$ with the corresponding eigenvalues $-n(n+1)$. The rotational harmonics $D_n^{j,k}$ are the matrix entries of the left regular representations of $SO(3)$, see [21, 41]. In particular, the rotation of a spherical harmonic satisfies

$$Y_n^k(Q^{-1}\boldsymbol{\xi}) = \sum_{j=-n}^{n} D_n^{j,k}(Q)\, Y_n^j(\boldsymbol{\xi}). \tag{6}$$

2.3 Singular value decomposition

Let $\mathscr{K}: X \to Y$ be a compact linear operator between the separable Hilbert spaces X and Y. A singular system $\{(u_n, v_n, \sigma_n) : n \in \mathbb{N}_0\}$ consists of an orthonormal basis $\{u_n\}_{n=0}^{\infty}$ of X, an orthonormal basis $\{v_n\}_{n=0}^{\infty}$ in the closed range of $\mathscr{K}$ and singular values $\sigma_n \to 0$ such that operator $\mathscr{K}$ can be diagonalized as

$$\mathscr{K}x = \sum_{n=0}^{\infty} \sigma_n \langle x, u_n \rangle v_n, \qquad x \in X.$$

If all singular values σ_n are nonzero, the operator $\mathscr{K}$ is injective and for $y = \mathscr{K}x$, we have

$$x = \sum_{n=0}^{\infty} \frac{\langle y, v_n \rangle}{\sigma_n} u_n.$$

The instability of an inverse problem can be characterized by the decay of the singular values. The problem of solving $\mathscr{K}x = y$ for x is called mildly ill-posed of degree $\alpha > 0$ if $\sigma_n \in \mathscr{O}(n^{-\alpha})$, cf. [8, Sec. 2.2].

3 Circle arcs

For any two points $\boldsymbol{\xi}, \boldsymbol{\zeta}$ on the sphere $\mathbb{S}^2$ that are not antipodal, there exists a shortest geodesic $\gamma(\boldsymbol{\xi}, \boldsymbol{\zeta})$ between $\boldsymbol{\xi}$ and $\boldsymbol{\zeta}$. This geodesic is an arc of the great circle that contains $\boldsymbol{\xi}$ and $\boldsymbol{\zeta}$.

The manifold of all great circle arcs is four-dimensional since they are determined by two points $\boldsymbol{\xi}, \boldsymbol{\zeta} \in \mathbb{S}^2$ and only coincide when $\boldsymbol{\xi}$ and $\boldsymbol{\zeta}$ are interchanged.
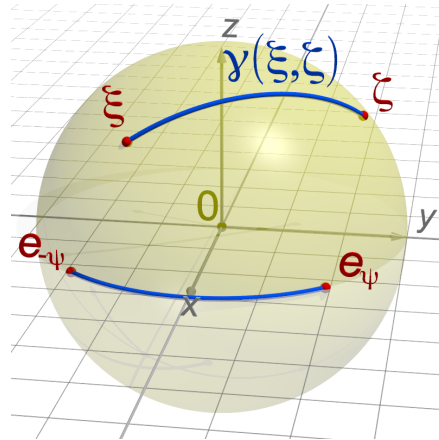
Fig. 1: Visualiation of the arc $\gamma(\boldsymbol{\xi}, \boldsymbol{\zeta})$

3.1 The arc transform

A great circle arc $\gamma(\boldsymbol{\xi},\boldsymbol{\zeta})$ can be parameterized by its length $2\psi = \arccos(\langle\boldsymbol{\xi},\boldsymbol{\zeta}\rangle)$ and a rotation $Q \in \mathrm{SO}(3)$ which is defined as follows. Let

$$\boldsymbol{e}_\varphi = (\cos\varphi, \sin\varphi, 0)^\top \in \mathbb{S}^2$$

be the point on the equator of $\mathbb{S}^2$ with latitude $\varphi \in \mathbb{R}$. Then there exists a unique rotation $Q \in \mathrm{SO}(3)$ such that $Q(\boldsymbol{\xi}) = \boldsymbol{e}_{-\psi}$ and $Q(\boldsymbol{\zeta}) = \boldsymbol{e}_\psi$. Such an arc γ and its rotation are depicted in Fig. 1. With this definition, the integral over the arc $\gamma(\boldsymbol{\xi},\boldsymbol{\zeta})$ may be rewritten as

$$\int_{\gamma(\boldsymbol{\xi},\boldsymbol{\zeta})} f(\boldsymbol{\eta})\,\mathrm{d}\boldsymbol{\eta} = \int_{Q\gamma(\boldsymbol{\xi},\boldsymbol{\zeta})} f(Q^{-1}\boldsymbol{\eta})\,\mathrm{d}\boldsymbol{\eta} = \int_{-\psi}^{\psi} f \circ Q^{-1}(\boldsymbol{e}_\varphi)\,\mathrm{d}\varphi.$$

This motivates the following definition of the arc transform

$$\begin{aligned}
\mathscr{A} &: C(\mathbb{S}^2) \to C(\mathrm{SO}(3) \times [0,\pi]), \\
\mathscr{A} f(Q,\psi) &= \int_{-\psi}^{\psi} f \circ Q^{-1}(\boldsymbol{e}_\varphi)\,\mathrm{d}\varphi.
\end{aligned} \tag{7}$$

The great circle arcs $\gamma(\boldsymbol{\xi},\boldsymbol{\zeta})$ and $\gamma(\boldsymbol{\zeta},\boldsymbol{\xi})$ are identical. This symmetry also holds for the operator $\mathscr{A}$. Using Euler angles, we have the identity

$$\mathscr{A} f(Q(\alpha,\beta,\gamma),\psi) = \mathscr{A} f(Q(2\pi - \alpha, \pi - \beta, \gamma + \pi), \psi),$$

where we assume the Euler angle γ as 2π-periodic.

3.2 Singular value decomposition of the arc transform

In the following, we use double factorials defined by $n!! = n(n-2)\cdots 2$ for n even or $n!! = n(n-2)\cdots 1$ for n odd and $0!! = (-1)!! = 1$. The next theorem shows how the arc transform $\mathscr{A}$ acts on spherical harmonics Y_n^k. The corresponding result for the parametrization in terms of the endpoints of an arc is found in [6, Appx. C], see also [3].

Theorem 3.1. *Let $n \in \mathbb{N}_0$ and $k \in \{-n,\dots,n\}$. Then*

$$\mathscr{A} Y_n^k(Q,\psi) = \sum_{j=-n}^{n} \widetilde{P}_n^j(0)\, D_n^{j,k}(Q)\, s_j(\psi), \tag{8}$$

where

$$s_j(\psi) = \begin{cases} 2\psi, & j = 0 \\ \frac{2\sin(j\psi)}{j}, & j \neq 0 \end{cases} \tag{9}$$

and

$$\widetilde{P}_n^j(0) = \begin{cases} (-1)^{\frac{n+j}{2}} \sqrt{\frac{2n+1}{4\pi} \frac{(n-j-1)!!(n+j-1)!!}{(n-j)!!(n+j)!!}}, & n+j \text{ even} \\ 0, & n+j \text{ odd.} \end{cases} \tag{10}$$

Proof. By (6), we obtain

$$\mathscr{A} Y_n^k(Q, \psi) = \int_{-\psi}^{\psi} Y_n^k(Q^{-1}(\boldsymbol{e}_\varphi)) = \sum_{j=-n}^{n} D_n^{j,k}(Q) \int_{-\psi}^{\psi} Y_n^j(\boldsymbol{e}_\varphi) \, d\varphi.$$

By the definition (3) of the spherical harmonics, we see that

$$\int_{-\psi}^{\psi} Y_n^j(\boldsymbol{e}_\varphi) \, d\varphi = \widetilde{P}_n^j(0) \int_{-\psi}^{\psi} e^{\mathrm{i}j\varphi} \, d\varphi = \widetilde{P}_n^j(0) \, s_j(\psi).$$

Hence,

$$\mathscr{A} Y_n^k(Q, \psi) = \sum_{j=-n}^{n} D_n^{j,k}(Q) \, \widetilde{P}_n^j(0) \, s_j(\psi).$$

Now we calculate $\widetilde{P}_n^j(0)$. By [23], $P_n^j(0) = 0$ if $n+j$ is odd and otherwise

$$P_n^j(0) = (-1)^{\frac{n+j}{2}} \frac{(n+j-1)!!}{(n-j)!!}.$$

Hence, we obtain by (2)

$$\widetilde{P}_n^j(0) = \sqrt{\frac{2n+1}{4\pi} \frac{(n-j)!}{(n+j)!}} (-1)^{\frac{n+j}{2}} \frac{(n+j-1)!!}{(n-j)!!}$$

$$= (-1)^{\frac{n+j}{2}} \sqrt{\frac{2n+1}{4\pi} \frac{(n-j-1)!!(n+j-1)!!}{(n-j)!!(n+j)!!}}$$

if $n+j$ is even, which implies (10). ∎

Lemma 3.2. *Let $n \in \mathbb{N}_0$ and $j \in \{-n, \ldots, n\}$. If $n+j$ is odd, then $\widetilde{P}_n^j(0) = 0$. Otherwise, we have*

$$\frac{2n+1}{2\pi^2 \sqrt{(n+1)^2 - j^2}} \leq \left| \widetilde{P}_n^j(0) \right|^2 \leq \frac{2n+1}{4\pi \sqrt{(n+1)^2 - j^2}}. \tag{11}$$

Furthermore, for $j \in \mathbb{N}_0$,

$$\lim_{\substack{n \to \infty \\ n+j \text{ even}}} \left| \widetilde{P}_n^j(0) \right| = \frac{1}{\pi}. \tag{12}$$

Proof. We first show that for $m \in \mathbb{N}$,

$$\sqrt{\frac{2}{\pi(2m+1)}} \leq \frac{(2m-1)!!}{(2m)!!} \leq \frac{1}{\sqrt{2m+1}}. \tag{13}$$

With the definition

$$u(m) = \left(\frac{(2m)!!}{(2m-1)!!}\right)^2 \frac{1}{2m+1}, \qquad m \in \mathbb{N}_0,$$

we see that $u(0) = 1$ and u is increasing because of $m \geq 1$ and

$$\frac{u(m)}{u(m-1)} = \frac{(2m)^2}{(2m-1)^2} \frac{2m-1}{2m+1} = \frac{(2m)^2}{(2m)^2-1} > 1.$$

That implies the right inequality of (13). Furthermore, Wallis' product states the convergence

$$u(m) = \frac{2}{1} \frac{2}{3} \frac{4}{3} \frac{4}{5} \frac{6}{5} \frac{6}{7} \cdots \frac{2m}{2m-1} \frac{2m}{2m+1} \longrightarrow \frac{\pi}{2} \tag{14}$$

for $m \to \infty$, see also [4]. This shows the left inequality of (13).

By (10) and (13), we obtain the upper bound

$$\left|\widetilde{P}_n^j(0)\right|^2 = \frac{2n+1}{4\pi} \frac{(n-j-1)!!}{(n-j)!!} \frac{(n+j-1)!!}{(n+j)!!} \leq \frac{2n+1}{4\pi} \frac{1}{\sqrt{n-j+1}} \frac{1}{\sqrt{n+j+1}}.$$

The lower bound follows analogously. Moreover, we have

$$\left|\widetilde{P}_{j+2m}^j(0)\right|^2 = \frac{2(j+2m)+1}{4\pi} \frac{(2m-1)!!}{(2m)!!} \frac{(2m+2j-1)!!}{(2m+2j)!!}.$$

Hence, Wallis product (14) shows that for $j \in \mathbb{N}_0$

$$\lim_{m\to\infty} \left|\widetilde{P}_{j+2m}^j(0)\right|^2 = \lim_{m\to\infty} \frac{2(j+2m)+1}{4\pi} \frac{2}{\pi} \frac{1}{\sqrt{2m+1}\sqrt{2m+2j+1}}$$

$$= \lim_{m\to\infty} \frac{2m+j+\frac{1}{2}}{\pi^2 \sqrt{(2m+j+1)^2-j^2}} = \frac{1}{\pi^2},$$

which proves the assertion. ∎

Next, we derive a singular value decomposition for the spherical arc transform. To this end, we define for $n \in \mathbb{N}_0$ and $k = -n, \ldots, n$ the functions $E_n^k \in L^2(\mathrm{SO}(3) \times [0, \pi])$ by

$$E_n^k(Q, \psi) = \sum_{j=-n}^n D_n^{j,k}(Q) \widetilde{P}_n^j(0) s_j(\psi), \qquad Q \in \mathrm{SO}(3), \ \psi \in [0, \pi]. \tag{15}$$

Theorem 3.3. *The operator $\mathscr{A} : L^2(\mathbb{S}^2) \to L^2(\mathrm{SO}(3) \times [0,\pi])$ is compact with the singular value decomposition*

$$\left\{ \left(Y_n^k, \, \widetilde{E}_n^k, \, \sigma_n \right) : n \in \mathbb{N}_0, \, k \in \{-n, \dots, n\} \right\},$$

with the singular values

$$\sigma_n = \left\| E_n^k \right\|_{L^2(\mathrm{SO}(3) \times [0,\pi])} = \sqrt{\frac{32\pi^3}{2n+1}} \sqrt{\frac{\pi^2}{3} \left| \widetilde{P}_n^0(0) \right|^2 + \sum_{j=1}^n \frac{1}{j^2} \left| \widetilde{P}_n^j(0) \right|^2} \qquad (16)$$

satisfying

$$\sqrt{\frac{16}{3}\pi^3} \le \sigma_n \sqrt{n+1} \le \sqrt{\frac{8}{3}\pi^4 + 4\pi^2}, \qquad \qquad n \text{ even,} \qquad (17)$$

$$4\sqrt{\pi} \le \sigma_n \sqrt{n+1} \le 2\pi \sqrt{\frac{4}{\sqrt{3}} + 1}, \qquad \qquad n \text{ odd,} \qquad (18)$$

and the orthonormal function system $\widetilde{E}_k^n = \sigma_n^{-1} E_n^k$, $n \in \mathbb{N}_0$, $k \in \{-n, \dots, n\}$ in $L^2(\mathrm{SO}(3) \times [0,\pi])$.

Proof. By the orthogonality (4) of the rotational harmonics, we have

$$\left\langle E_n^k, E_{n'}^{k'} \right\rangle_{L^2(\mathrm{SO}(3) \times [0,\pi])}$$

$$= \sum_{j=-n}^n \sum_{j'=-n'}^{n'} \widetilde{P}_n^j(0) \, \widetilde{P}_{n'}^{j'}(0) \int_{\mathrm{SO}(3)} D_n^{j,k}(Q) \overline{D_{n'}^{j',k'}(Q)} \, \mathrm{d}Q \int_0^\pi s_j(\psi) \, s_{j'}(\psi) \, \mathrm{d}\psi$$

$$= \sum_{j=-n}^n \sum_{j'=-n'}^{n'} \frac{8\pi^2}{2n+1} \delta_{nn'} \, \delta_{kk'} \, \delta_{jj'} \, \widetilde{P}_n^j(0) \, \widetilde{P}_{n'}^{j'}(0) \int_0^\pi s_j(\psi) \, s_{j'}(\psi) \, \mathrm{d}\psi$$

$$= \delta_{nn'} \, \delta_{kk'} \sum_{j=-n}^n \frac{8\pi^2}{2n+1} \left| \widetilde{P}_n^j(0) \right|^2 \int_0^\pi s_j(\psi)^2 \, \mathrm{d}\psi$$

$$= \delta_{nn'} \, \delta_{kk'} \frac{8\pi^2}{2n+1} \sum_{j=-n}^n \left| \widetilde{P}_n^j(0) \right|^2 \begin{cases} \frac{4\pi^3}{3}, & j = 0 \\ \frac{2\pi}{j^2}, & j \ne 0. \end{cases}$$

This shows that the functions $\mathscr{A} Y_n^k$ are orthogonal in the space $L^2(\mathrm{SO}(3) \times [0,\pi])$ and have the norm

$$\left\| E_n^k \right\|_{L^2(\mathrm{SO}(3) \times [0,\pi])}^2 = \frac{8\pi^2}{2n+1} \sum_{j=-n}^n \left| \widetilde{P}_n^j(0) \right|^2 \begin{cases} \frac{4\pi^3}{3}, & j = 0 \\ \frac{2\pi}{j^2}, & j \ne 0. \end{cases}$$

$$= \frac{16\pi^3}{2n+1} \left(\frac{2\pi^2}{3} \left| \widetilde{P}_n^0(0) \right|^2 + 2 \sum_{j=1}^n \frac{1}{j^2} \left| \widetilde{P}_n^j(0) \right|^2 \right),$$

where we used that $\left|\widetilde{P}_n^j(0)\right| = \left|\widetilde{P}_n^{-j}(0)\right|$. In order to prove that $\mathscr{A}$ is compact, we show that the singular values σ_n decay for $n \to \infty$. We have by Lemma 3.2 for $n = 2m$ even

$$\sigma_{2m}^2 \leq 4\pi^2 \left(\frac{2\pi^2}{3} \frac{1}{2m+1} + 2 \sum_{j=1}^{m} \frac{1}{(2j)^2} \frac{1}{\sqrt{(2m+1)^2 - (2j)^2}} \right).$$

Replacing the sum by an integral, we estimate for n even

$$2 \sum_{j=1}^{m} \frac{1}{(2j)^2} \frac{1}{\sqrt{(2m+1)^2 - (2j)^2}} \leq 2 \int_{1/2}^{m+1/2} \frac{1}{(2j)^2} \frac{1}{\sqrt{(2m+1)^2 - (2j)^2}} \, \mathrm{d}j$$

$$= 2 \left[-\frac{\sqrt{(2m+1)^2 - (2j)^2}}{2j(2m+1)^2} \right]_{1/2}^{m+1/2}$$

$$= 2 \frac{\sqrt{m^2 + m}}{(2m+1)^2} \leq \frac{1}{2m+1},$$

where we made use of the convexity of the integrand. Hence,

$$\sigma_{2m}^2 \leq 4\pi^2 \left(\frac{2\pi^2}{3} \frac{1}{2m+1} + \frac{1}{2m+1} \right) = 4\pi^2 \left(\frac{2\pi^2}{3} + 1 \right) \frac{1}{2m+1}.$$

For odd $n = 2m - 1$, we proceed analogously. We have

$$\sigma_{2m-1}^2 \leq 8\pi^2 \sum_{j=1}^{m} \frac{1}{(2j-1)^2} \frac{1}{\sqrt{(2m)^2 - (2j-1)^2}}.$$

Note that, for the estimation of the sum by an integral, we extract the summand for $j = 1$

$$\sigma_{2m-1}^2 \leq 8\pi^2 \left(\frac{1}{\sqrt{(2m)^2 - 1}} + \int_1^{m+1/2} \frac{1}{(2j-1)^2} \frac{1}{\sqrt{(2m)^2 - (2j-1)^2}} \, \mathrm{d}j \right)$$

$$= 8\pi^2 \left(\frac{1}{\sqrt{(2m)^2 - 1}} + \frac{\sqrt{(2m)^2 - 1}}{2(2m)^2} \right)$$

$$\leq 8\pi^2 \left(\frac{2}{\sqrt{3} \, 2m} + \frac{1}{2(2m)} \right) = 4\pi^2 \left(\frac{4}{\sqrt{3}} + 1 \right) \frac{1}{2m}.$$

For the lower bound of the singular values, we also use Lemma 3.2. For even n, we extract the summand $j = 0$ and obtain

$$\sigma_n^2 = \frac{16\pi^3}{2n+1}\left(\frac{2\pi^2}{3}\left|\widetilde{P}_n^0(0)\right|^2 + 2\sum_{j=1}^{n}\frac{1}{j^2}\left|\widetilde{P}_n^j(0)\right|^2\right)$$

$$\geq \frac{32\pi^5}{3(2n+1)}\left|\widetilde{P}_n^0(0)\right|^2 \geq \frac{16\pi^3}{3(n+1)}.$$

For odd n, we extract the summand $j = 1$ and obtain

$$\sigma_n^2 \geq \frac{32\pi^3}{2n+1}\left|\widetilde{P}_n^1(0)\right|^2 \geq \frac{16\pi}{\sqrt{(n+1)^2-1}} \geq \frac{16\pi}{n+1}.$$

∎

The singular values σ_n decay with rate $n^{-1/2}$. This is the same asymptotic decay rate as of the eigenvalues of the Funk–Radon transform, cf. [39].

4 Special cases

The recovery of a function f from the arc integrals $\mathscr{A}f$ is overdetermined considered we have full data. In the following subsections, we are going to examine some special cases, where we can reconstruct f from integrals only along certain arcs.

4.1 Arcs starting in a fixed point

As a simple example, we fix one endpoint of the arcs. Without loss of generality, we assume that this endpoint is the north pole. The arc connecting the north pole e^3 and an arbitrary other point $\boldsymbol{\xi}(\varphi, \vartheta) \in \mathbb{S}^2$ is given by

$$\gamma(e^3, \boldsymbol{\xi}(\varphi, \vartheta)) = \{\boldsymbol{\eta}(\varphi, \rho) \in \mathbb{S}^2 : \rho \in [0, \vartheta]\}.$$

Since, with $Q = Q\left(\frac{\vartheta}{2}, \frac{\pi}{2}, \frac{3\pi}{2} - \varphi\right) \in \mathrm{SO}(3)$, we have $Qe^3 = e_{\frac{\vartheta}{2}}$ and $Q\boldsymbol{\xi} = e_{-\frac{\vartheta}{2}}$. The restriction $\mathscr{B}\colon C(\mathbb{S}^2) \to C(\mathbb{S}^2)$ of the operator $\mathscr{A}$ to these arcs satisfies

$$\mathscr{B}f(\boldsymbol{\xi}(\varphi, \vartheta)) = \mathscr{A}f\left(Q\left(\tfrac{\vartheta}{2}, \tfrac{\pi}{2}, \tfrac{3\pi}{2} - \varphi\right), \tfrac{\vartheta}{2}\right) = \int_0^{\vartheta} f(\boldsymbol{\eta}(\varphi, \rho))\,\mathrm{d}\rho.$$

If f is additionally differentiable, it can be recovered from $\mathscr{B}f$ by

$$f(\boldsymbol{\xi}(\varphi, \vartheta)) = \frac{\mathrm{d}}{\mathrm{d}\vartheta}\mathscr{B}f(\boldsymbol{\xi}(\varphi, \vartheta)).$$

The following more general result for injectivity is due to [2, Theorem 4.4.1]. Its proof uses a similar idea combined with an extension by density.

Proposition 4.1. *Let S be an open subset of $\mathbb{S}^2$ and $A, B \subset S$ nonempty sets with $\overline{A \cup B} = \overline{S}$. If $f \in C(\mathbb{S}^2)$ and*

$$\int_{\gamma(\boldsymbol{\xi}, \boldsymbol{\zeta})} f(\boldsymbol{\eta}) \, d\boldsymbol{\eta} = 0 \qquad \text{for all } \boldsymbol{\xi} \in A, \boldsymbol{\zeta} \in B,$$

then $f \equiv 0$ on S.

For $A = \{\boldsymbol{e}^3\}$ and $B = \mathbb{S}^2$, we have the arcs starting in the north pole.

4.2 Recovery of local functions

A subset $\Omega \subset \mathbb{S}^2$ is called convex if for any two points $\boldsymbol{\xi}, \boldsymbol{\eta} \in \Omega$ the geodesic arc $\gamma(\boldsymbol{\xi}, \boldsymbol{\eta})$ is contained in Ω. We denote by $\partial\Omega$ the boundary of Ω.

Theorem 4.2. *Let $f \in C(\mathbb{S}^2)$ and Ω be a convex subset of $\mathbb{S}^2$ whose closure $\overline{\Omega}$ is strictly contained in a hemisphere, i.e., there exists a $\boldsymbol{\zeta} \in \mathbb{S}^2$ such that $\langle \boldsymbol{\xi}, \boldsymbol{\zeta} \rangle > 0$ for all $\boldsymbol{\xi} \in \overline{\Omega}$. If*

$$\int_{\gamma(\boldsymbol{\xi}, \boldsymbol{\eta})} f(\boldsymbol{\eta}) \, d\boldsymbol{\eta} = 0 \qquad \text{for all } \boldsymbol{\xi}, \boldsymbol{\eta} \in \partial\Omega, \tag{19}$$

then $f = 0$ on Ω.

Proof. Without loss of generality, we assume that $\overline{\Omega}$ is strictly contained in the northern hemisphere, i.e., we have $\xi_3 > 0$ for all $\boldsymbol{\xi} \in \overline{\Omega}$. We define the restriction of f to $\overline{\Omega}$ by

$$f_\Omega(\boldsymbol{\xi}) = \begin{cases} f(\boldsymbol{\xi}), & \boldsymbol{\xi} \in \overline{\Omega} \\ 0, & \boldsymbol{\xi} \in \mathbb{S}^2 \setminus \overline{\Omega} \end{cases}$$

Since $\gamma(\boldsymbol{\xi}, \boldsymbol{\eta}) \subset \overline{\Omega}$ for all $\boldsymbol{\xi}, \boldsymbol{\eta} \in \partial\Omega$, the function f_Ω also satisfies (19).

For $\boldsymbol{\xi} \in \mathbb{S}^2$, denote with $\boldsymbol{\xi}^\perp = \{\boldsymbol{\eta} \in \mathbb{S}^2 : \langle \boldsymbol{\xi}, \boldsymbol{\eta} \rangle = 0\}$ the great circle perpendicular to $\boldsymbol{\xi}$. We show that the Funk–Radon transform

$$\mathscr{F} f_\Omega(\boldsymbol{\xi}) = \int_{\boldsymbol{\xi}^\perp \cap \overline{\Omega}} f_\Omega(\boldsymbol{\eta}) \, d\boldsymbol{\eta} + \int_{\boldsymbol{\xi}^\perp \setminus \overline{\Omega}} f_\Omega(\boldsymbol{\eta}) \, d\boldsymbol{\eta} \tag{20}$$

vanishes everywhere. The second summand of (20) vanishes because f_Ω is zero outside $\overline{\Omega}$ by definition. If $\boldsymbol{\xi}^\perp \cap \overline{\Omega}$ is not empty, there exist two points $\boldsymbol{\eta}^1, \boldsymbol{\eta}^2 \in \partial\Omega$ such that $\gamma(\boldsymbol{\eta}^1, \boldsymbol{\eta}^2) = \boldsymbol{\xi}^\perp \cap \overline{\Omega}$, which shows that also the first summand of (20) vanishes. Hence, $\mathscr{F} f_\Omega = 0$ on $\mathbb{S}^2$. Since the Funk–Radon transform $\mathscr{F}$ is injective for even functions, we see that f_Ω must be odd. Since f_Ω is supported strictly inside the northern hemisphere, so f_Ω must be the zero function. By the construction, we see that $f(\boldsymbol{\xi})$ vanishes for all $\boldsymbol{\xi} \in \Omega$. ∎

An analogue to Theorem 4.2 for Ω being the northern hemisphere and the arcs being half circles is shown in [36].

4.3 Arcs with fixed length

In the following, we consider circle arcs with fixed length ψ. To this end, we define the restriction

$$\mathscr{A}_\psi(Q) = \mathscr{A}(Q, \psi).$$

Theorem 4.3. *Let $\psi \in (0, \pi)$ be fixed. The operator $\mathscr{A}_\psi \colon L^2(\mathbb{S}^2) \to L^2(\mathrm{SO}(3))$ has the singular value decomposition*

$$\left\{ \left(Y_n^k, Z_{n,\psi}^k, \mu_n(\psi) \right) : n \in \mathbb{N}_0, k \in \{-n, \ldots, n\} \right\},$$

with the singular values

$$\mu_n(\psi) = \sqrt{\sum_{j=-n}^{n} \frac{8\pi^2}{2n+1} \left| \widetilde{P}_n^j(0) \right|^2 s_j(\psi)^2} \qquad (21)$$

and the singular functions

$$Z_{n,\psi}^k = \frac{\mathscr{A}_\psi Y_n^k}{\mu_n(\psi)} = \frac{1}{\mu_n(\psi)} \sum_{j=-n}^{n} \widetilde{P}_n^j(0) \, s_j(\psi) \, D_n^{j,k}.$$

In particular, $\mathscr{A}_\psi$ is injective.

Proof. Let $\psi \in (0, \pi)$ be fixed, $n \in \mathbb{N}_0$ and $k \in \{-n, \ldots, n\}$. We have by (8)

$$\left\langle \mathscr{A}_\psi Y_n^k, \mathscr{A}_\psi Y_{n'}^{k'} \right\rangle_{L^2(\mathrm{SO}(3))}$$

$$= \sum_{j=-n}^{n} \sum_{j'=-n'}^{n'} \int_{\mathrm{SO}(3)} D_n^{j,k}(Q) \overline{D_{n'}^{j',k'}(Q)} \, \widetilde{P}_n^j(0) \, \widetilde{P}_{n'}^{j'}(0) \, s_j(\psi) \, s_{j'}(\psi) \, \mathrm{d}Q$$

$$= \sum_{j=-n}^{n} \sum_{j'=-n'}^{n'} \frac{8\pi^2}{2n+1} \delta_{nn'} \, \delta_{kk'} \, \delta_{jj'} \, \widetilde{P}_n^j(0) \, \widetilde{P}_{n'}^{j'}(0) \, s_j(\psi) \, s_{j'}(\psi)$$

$$= \delta_{nn'} \delta_{kk'} \sum_{j=-n}^{n} \frac{8\pi^2}{2n+1} \left| \widetilde{P}_n^j(0) \right|^2 s_j(\psi)^2.$$

For the injectivity, we check that the singular values $\mu_n(\psi)$ do not vanish for each $n \in \mathbb{N}_0$. We have $\widetilde{P}_n^j(0) = 0$ if and only if $n - j$ is odd. Furthermore, the definition of s_j in (9) shows that $s_0(\psi) = 2\psi$ vanishes if and only if $\psi = 0$ and $s_1(\psi) = 2\sin(\psi)$ vanishes if and only if ψ is an integer multiple of π. Hence, the functions $\mathscr{A} Y_n^k$ are

also orthogonal in the space $L^2(SO(3))$. ∎

Theorem 4.4. *The singular values $\mu_n(\psi)$ of $\mathscr{A}_\psi$ satisfy for odd $n = 2m - 1$*

$$\lim_{m\to\infty} \frac{4m-1}{4} \mu_{2m-1}(\psi)^2 = \begin{cases} 4\pi\psi, & \psi \in [0, \frac{\pi}{2}] \\ 4\pi^2 - 4\pi\psi, & \psi \in [\frac{\pi}{2}, \pi], \end{cases} \tag{22}$$

and for even $n = 2m$

$$\lim_{m\to\infty} \frac{4m+1}{4} \mu_{2m}(\psi)^2 = \begin{cases} 4\pi\psi, & \psi \in [0, \frac{\pi}{2}] \\ 12\pi\psi - 4\pi^2, & \psi \in [\frac{\pi}{2}, \pi]. \end{cases} \tag{23}$$

Proof. We first show (22). Let $m \in \mathbb{N}$. We have by (21)

$$\frac{4m-1}{4} \mu_{2m-1}(\psi)^2 = 16\pi^2 \sum_{j=1}^{m} \left| \widetilde{P}_{2m-1}^{2j-1}(0) \right|^2 \frac{\sin^2((2j-1)\psi)}{(2j-1)^2}.$$

We denote by $v(\psi) = 4\pi \left(\frac{\pi}{2} - \left| \psi - \frac{\pi}{2} \right| \right)$ the right-hand side of (22). The Fourier cosine series of v reads by [14, 1.444]

$$16 \sum_{k=1}^{\infty} \frac{\sin((2k-1)\psi)^2}{(2k-1)^2} = 16 \sum_{k=1}^{\infty} \frac{1 - \cos((2k-1)2\psi)}{2(2k-1)^2} = v(\psi), \qquad \psi \in [0, \pi].$$

We have

$$\left\| \frac{4m-1}{4} \mu_{2m-1}^2 - v \right\|_{C([0,\pi])} = \left\| 16 \sum_{j=1}^{\infty} \frac{\pi^2 \left| \widetilde{P}_{2m-1}^{2j-1}(0) \right|^2 - 1}{(2j-1)^2} \sin^2((2j-1)\psi) \right\|_{C([0,\pi])}$$

$$\leq \sum_{j=1}^{\infty} \frac{16 \left| \pi^2 \left| \widetilde{P}_{2m-1}^{2j-1}(0) \right|^2 - 1 \right|}{(2j-1)^2}. \tag{24}$$

We show that (24) goes to zero for $m \to \infty$, which then implies (22). By (12), we see that $\pi^2 |\widetilde{P}_{2m-1}^{2j-1}(0)|^2$ converges to 1 for $m \to \infty$. Using the singular values (16) together with their bound (18), we obtain the following summable majorant of (24):

$$\sum_{j=1}^{\infty} \frac{16\pi^2 \left| \widetilde{P}_{2m-1}^{2j-1}(0) \right|^2}{(2j-1)^2} \leq \frac{4m-1}{2\pi} \sigma_{2m-1}^2 \leq 2\pi \frac{4m-1}{m} \left(\frac{4}{\sqrt{3}} + 1 \right).$$

Hence, the sum (24) converges to 0 for $m \to \infty$ by the dominated convergence theorem of Lebesgue.

In the second part, we show (23) for the odd singular values. Let $m \in \mathbb{N}$. We have

$$\frac{4m+1}{4}\,\mu_{2m}(\psi)^2 = 8\pi^2\left|\widetilde{P}_{2m}^0(0)\right|^2\psi^2 + 4\pi^2\sum_{k=1}^{m}\left|\widetilde{P}_{2m}^{2k}(0)\right|^2\frac{\sin^2(2k\psi)}{k^2}. \qquad (25)$$

We examine both summands on the right side of (25). The first summand converges due to (12):

$$\lim_{m\to\infty}8\pi^2\left|\widetilde{P}_{2m}^0(0)\right|^2\psi^2 = 8\psi^2.$$

We denote the second summand of (25) by

$$\lambda_m(\psi) = 4\pi^2\sum_{k=1}^{m}\left|\widetilde{P}_{2m}^{2k}(0)\right|^2\frac{\sin^2(2k\psi)}{k^2}$$

and define λ by the following Fourier cosine series, see [14, 1.443],

$$\lambda(\psi) = \sum_{k=1}^{\infty}\frac{\sin^2(2k\psi)}{k^2} = \sum_{k=1}^{\infty}\frac{1-\cos(4k\psi)}{2k^2} = \begin{cases} -2\psi^2+\pi\psi, & \psi\in[0,\frac{\pi}{2}) \\ -2\psi^2+3\pi\psi-\pi^2, & \psi\in[\frac{\pi}{2},\pi). \end{cases}$$

We have

$$\|\lambda_m-\lambda\|_{C([0,\pi])} = \left\|\sum_{k=1}^{\infty}\frac{\pi^2\left|\widetilde{P}_{2m}^{2k}(0)\right|^2-1}{k^2}\sin^2(2k\psi)\right\|_{C([0,\pi])}$$

$$\leq \sum_{k=1}^{\infty}\frac{\left|\pi^2\left|\widetilde{P}_{2m}^{2k}(0)\right|^2-1\right|}{(2j-1)^2}.$$

As in the first part of the proof, we see with (17) that the last sum goes to 0 for $m\to\infty$, which proves (23). ∎

Remark 4.5. Theorem 4.4 shows that the singular values $\mu_n(\psi)$ decay with the same asymptotic rate of $n^{-1/2}$ as σ_n from Theorem 3.3. For $\psi < \frac{\pi}{2}$, the singular values $(n+\frac{1}{2})\mu_n(\psi)^2$ for even and odd n converge to the same limit. However, for $\psi > \frac{\pi}{2}$, the singular values for even n become larger than the ones for odd n. This might be explained by the fact that for odd n, the spherical harmonics Y_n^k are odd and integrating them along a circle arc with length 2ψ, which is longer than a half-circle, yields some cancellation. In the limiting case $\psi = \pi$, which is not covered by Theorem 4.3, $\mathscr{A}_\pi$ corresponds to the Funk–Radon transform, which is injective only for even functions and vanishes on odd functions. This behavior is illustrated in Fig. 2. □

Remark 4.6. Since the rotation group SO(3) is three-dimensional, the inversion of the arc transform $\mathscr{A}_\psi$ with fixed length is still overdetermined.

In the case $\psi = \frac{\pi}{2}$, we have the integrals along all half circles. The injectivity of the arc transform for half circles was shown in [18]. The restriction of the arc trans-
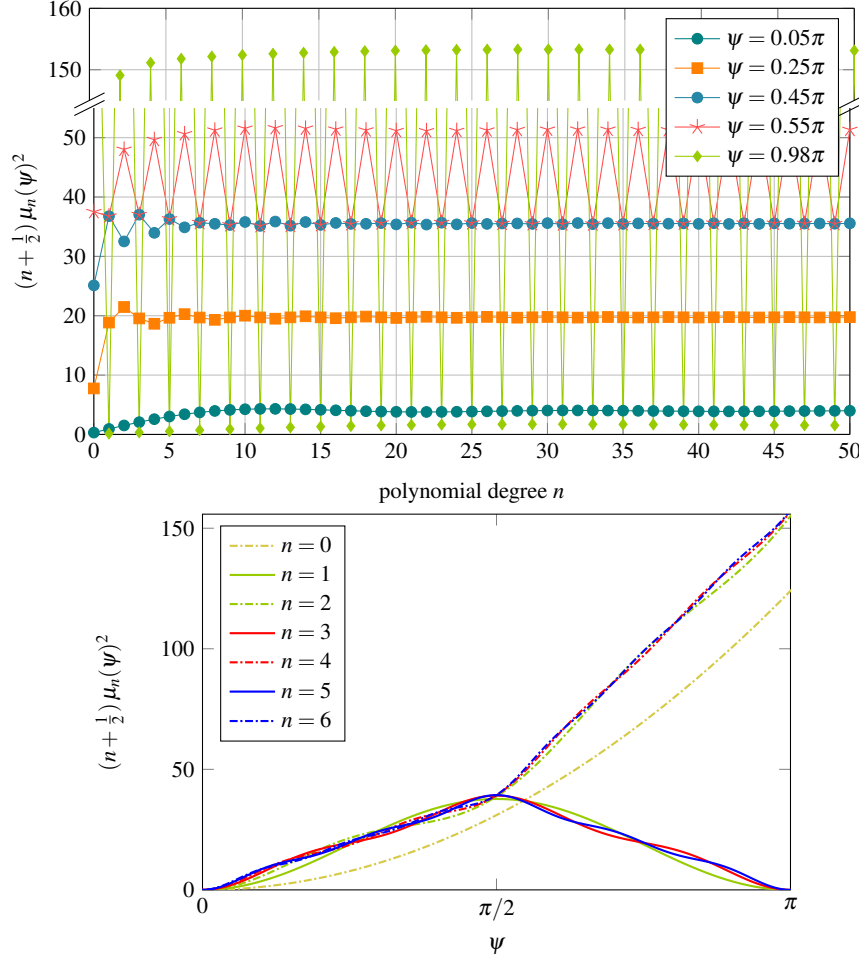
Fig. 2: The (normalized) singular values $(n + \frac{1}{2}) \mu_n(\psi)^2$. Top: dependency on the degree n. Note the oscillation for $\psi > \frac{\pi}{2}$. Bottom: dependency on the arc-length ψ (dashed lines correspond to even n).

form to all half circles that are subsets of either the upper or the lower hemisphere is still injective, see [36]. This is because every function that is supported in the upper (lower) hemisphere can be uniquely reconstructed by its Funk–Radon transform, which then integrates only over the half circles in the upper (lower) hemisphere. $\square$

The singular value decomposition from Theorem 4.3 allows us to reconstruct a function $f \in L^2(\mathbb{S}^2)$ given $g = \mathscr{A}_\psi f$.

Theorem 4.7. *Let $f \in L^2(\mathbb{S}^2)$ and $g = \mathscr{A}_\psi f \in L^2(\mathrm{SO}(3))$. Then f can be reconstructed from the rotational Fourier coefficients $\hat{g}_n^{j,k}$ given in* (5) *by*

$$f = \sum_{n=0}^{\infty} \sum_{k=-n}^{n} \frac{\sum_{j=-n}^{n} \widetilde{P}_n^j(0)\, s_j(\psi)\, \hat{g}_n^{j,k}}{\sum_{j=-n}^{n} \widetilde{P}_n^j(0)^2\, s_j(\psi)^2}\, Y_n^k. \tag{26}$$

Proof. We have by Theorem 4.3 for the spherical Fourier coefficients

$$\hat{f}_n^k = \frac{1}{\mu_n(\psi)} \left\langle g, Z_{n,\psi}^k \right\rangle_{L^2(\mathrm{SO}(3))}$$

$$= \frac{1}{\mu_n(\psi)^2} \sum_{j=-n}^{n} \widetilde{P}_n^j(0)\, s_j(\psi) \left\langle g, D_n^{j,k} \right\rangle_{L^2(\mathrm{SO}(3))}.$$

The assertion follows by (5) and (21).   ∎

Remark 4.8. A big advantage of using the singular value decomposition for inversion is that it is straightforward to apply Tikhnov-type regularization or the mollifier method [27], which both correspond to a multiplication of the summands in the inversion formula (26) with some filter coefficients c_n, cf. [22]. We obtain

$$f_c = \sum_{n=0}^{\infty} \sum_{k=-n}^{n} c_n \frac{\sum_{j=-n}^{n} \widetilde{P}_n^j(0)\, s_j(\psi)\, \hat{g}_n^{j,k}}{\sum_{j=-n}^{n} \widetilde{P}_n^j(0)^2\, s_j(\psi)^2}\, Y_n^k. \tag{27}$$

Filter coefficients corresponding to Pinsker estimators are optimal for functions in certain Sobolev spaces, cf. [9]. They were applied to the Funk–Radon transform in [22].   □

5 Numerical tests

We consider the arc transform $\mathscr{A}_\psi$ with fixed length $\psi \in (0,\pi)$ as in Section 4.3.

5.1 Forward algorithm

For given $f \in C(\mathbb{S}^2)$, we want to compute the arc transform $\mathscr{A}_\psi f(Q_m)$ at points $Q_m \in \mathrm{SO}(3)$, $m = 1,\ldots,M$. In order to derive an algorithm, we assume that $f \in \mathscr{P}_N(\mathbb{S}^2)$ is a polynomial. We compute the spherical Fourier coefficients

$$\hat{f}_n^k = \int_{\mathbb{S}^2} f(\boldsymbol{\xi})\, \overline{Y_n^k(\boldsymbol{\xi})}\, \mathrm{d}\boldsymbol{\xi}, \qquad n = 0,\ldots,N,\; k = -n,\ldots,n,$$

with a quadrature rule on $\mathbb{S}^2$ that is exact for polynomials of degree $2N$. The computation of the spherical Fourier coefficients $\hat{f}_n^k$ can be done with the adjoint NFSFT (Nonequispaced Fast Spherical Fourier Transform) algorithm [26] in

$\mathcal{O}(N^2 \log^2 N^2 + M)$ steps. Then, by (8),

$$\mathscr{A}_\psi f(Q_m) = \sum_{n=0}^{N} \sum_{j,k=-n}^{n} \hat{f}_n^k \widetilde{P}_n^j(0) \, s_j(\psi) \, D_n^{j,k}(Q), \qquad m = 1,\ldots,M, \qquad (28)$$

is a discrete rotational Fourier transform of degree N, which can be computed with the NFSOFT (Nonequispaced Fast SO(3) Fourier Transform) algorithm [32] in $\mathcal{O}(M + N^3 \log^2 N)$ steps. Implementations of both NFSFT and NFSOFT are contained in the NFFT library [24].

A simple alternative for the computation of $\mathscr{A}_\psi f$ is the following quadrature with K equidistant nodes

$$\mathscr{A}_\psi f(Q) \approx \frac{2\psi}{K} \sum_{i=1}^{K} f\left(Q^{-1}\left(e_{\rho_i}\right)\right), \qquad \rho_i = \frac{2i-1-K}{K}\,\psi. \qquad (29)$$

Computing $\mathscr{A}_\psi f(Q_m)$ for $m = 1,\ldots,M$ with the quadrature rule (29) requires $\mathcal{O}(KM)$ operations. Hence, for a high number M of evaluation nodes, the NFSOFT-based algroithm is faster than the quadrature based on (29).
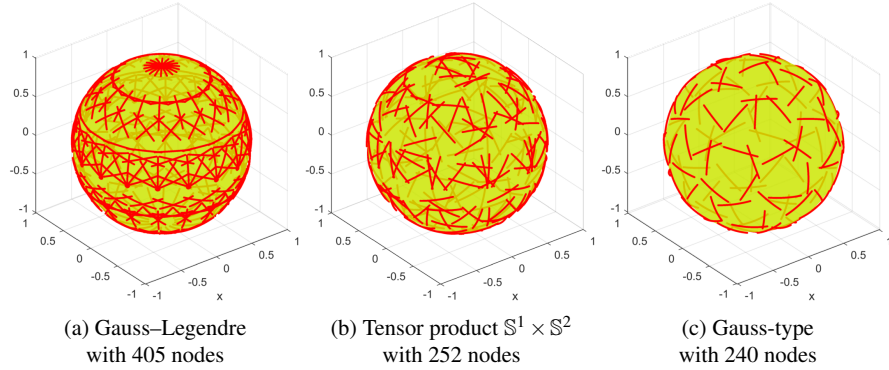
5.2 Inversion

(a) Gauss–Legendre with 405 nodes

(b) Tensor product $\mathbb{S}^1 \times \mathbb{S}^2$ with 252 nodes

(c) Gauss-type with 240 nodes

Fig. 3: Circle arcs $\gamma(Q_m, 0.2)$ corresponding to quadrature nodes $Q_m \in \mathrm{SO}(3)$, all quadrature formulas are exact for all rotational harmonics $D_n^{j,k}$ of degree $n \le 8$.

We test the inversion from Theorem 4.7. Let $g = \mathscr{A}_\psi f$. For the computation of the rotational Fourier coefficients $\hat{g}_n^{j,k}$, $n = 0,\ldots,N$, $j,k = -n,\ldots,n$, we use a quadrature formula

$$\hat{g}_n^{j,k} = \int_{\mathrm{SO}(3)} g(Q)\, \overline{D_n^{j,k}(Q)}\, \mathrm{d}Q \approx \sum_{m=1}^{M} w_m\, g(Q_m)\, \overline{D_n^{j,k}(Q_m)} \tag{30}$$

with nodes $Q_m \in \mathrm{SO}(3)$ and weights $w_m > 0$, $m = 1,\dots,M$. Again, we assume that $f \in \mathscr{P}_N(\mathbb{S}^2)$, which implies $\hat{g}_n^{j,k} = 0$ for $n > N$. Hence, (30) holds with equality if the quadrature integrates rotational harmonics up to degree $2N$ exactly. There are different ways to obtain such exact quadrature formulas on $\mathrm{SO}(3)$. In a tensor product approach, we use Gauss–Legendre quadrature in $\cos\beta$ and a trapezoidal rule in both α and γ. We can also write $\mathrm{SO}(3) \sim \mathbb{S}^1 \times \mathbb{S}^2$ and pair a trapezoidal rule on $\mathbb{S}^1$ in α with a quadrature on $\mathbb{S}^2$ with azimuth γ and polar angle β, see [17]. Furthermore, Gauss-type quadratures on $\mathrm{SO}(3)$ that are exact up to machine precision were computed in [16]. In Fig. 3, one can see the circle arcs corresponding to different quadrature rules on $\mathrm{SO}(3)$, namely Gauss–Legendre nodes (Fig. 3a), the tensor product of $\mathbb{S}^1 \times \mathbb{S}^2$ (Fig. 3b) and a Gauss-type quadrature on $\mathrm{SO}(3)$ (Fig. 3c). We used Gauss-type quadratures on both $\mathbb{S}^2$ and $\mathrm{SO}(3)$ from [15]. Note that because of the symmetry of the Gauss-type quadrature on $\mathrm{SO}(3)$ we used in Fig 3c, every arc corresponds to two quadrature nodes on $\mathrm{SO}(3)$.

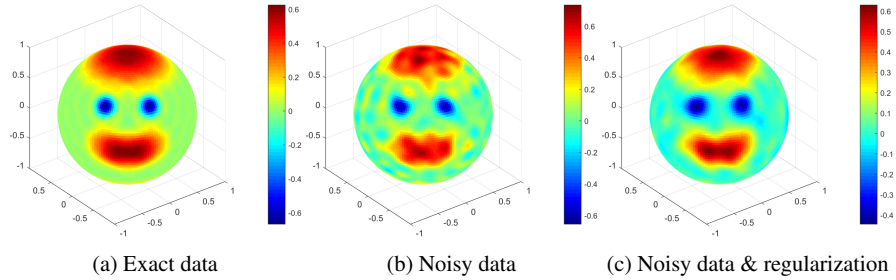(a) Exact data   (b) Noisy data   (c) Noisy data & regularization

Fig. 4: Reconstruction of a spherical test function f for degree $N = 22$, $\psi = 0.7$ and a tensor product $\mathbb{S}^1 \times \mathbb{S}^2$ quadrature ($M = 30240$).

The reconstruction formula (26) becomes the discrete rotational Fourier transform

$$f = \sum_{n=0}^{N} \sum_{k=-n}^{n} \frac{\sum_{j=-n}^{n} \widetilde{P}_n^j(0)\, s_j(\psi)\, \hat{g}_n^{j,k}}{\sum_{j=-n}^{n} \widetilde{P}_n^j(0)^2\, s_j(\psi)^2}\, Y_n^k.$$

In Fig. 4, we compare the reconstruction results, where we use an artificial test function, the parameter $N = 22$ and the tensor product of a trapezoidal rule on $\mathbb{S}^1$ with a Gauss-type quadrature on $\mathbb{S}^2$ from [15]. The resulting $\mathrm{SO}(3)$ quadrature uses $M = 30240$ nodes and is exact for degree 44. We first perform the inversion without any noise in the data. The reconstruction has an RMSE (root mean square error) of 0.0338. Then we add Gaussian white noise with a standard deviation of 0.2 to the data $\mathscr{A}_\psi f(Q_m)$ and achieve an RMSE of 0.2272. Even though we did not perform any regularization, the reconstruction from noisy data still looks considerably well. This might be explained by the fact that the inverse arc transform with fixed

opening angle and full $SO(3)$ data is still an overdetermined problem. Applying the regularization (27) truncated to degree $n \le N$ with filter coefficients from [22] yields a smaller RMSE of 0.1393.

References

1. A. Abouelaz and R. Daher. Sur la transformation de Radon de la sphère S^d. *Bull. Soc. math. France*, 121(3):353–382, 1993.
2. A. Amirbekyan. *The application of reproducing kernel based spline approximation to seismic surface and body wave tomography: theoretical aspects and numerical results*. PhD thesis, Technische Universität Kaiserslautern, 2007.
3. A. Amirbekyan, V. Michel, and F. J. Simons. Parametrizing surface wave tomographic models with harmonic spherical splines. *Geophys. J. Int.*, 174(2):617–628, 2008.
4. F. L. Bauer. Remarks on Stirling's formula and on approximations for the double factorial. *Math. Intelligencer*, 29(2):10–14, 2007.
5. R. Daher. Un théorème de support pour une transformation de Radon sur la sphère S^d. *C. R. Acad. Sci. Paris*, 332(9):795–798, 2001.
6. F. Dahlen and J. Tromp. *Theoretical Global Seismology*. Princeton University Press, 1998.
7. F. Dai and Y. Xu. *Approximation Theory and Harmonic Analysis on Spheres and Balls*. Springer Monographs in Mathematics. Springer, New York, 2013.
8. H. W. Engl, M. Hanke, and A. Neubauer. *Regularization of inverse problems*, volume 375 of *Mathematics and Its Applications*. Kluwer Academic Publishers, 1996.
9. D. Fournier, L. Gizon, M. Holzke, and T. Hohage. Pinsker estimators for local helioseismology: inversion of travel times for mass-conserving flows. *Inverse Problems*, 32(10):105002, 2016.
10. W. Freeden, T. Gervens, and M. Schreiner. *Constructive Approximation on the Sphere*. Oxford University Press, Oxford, 1998.
11. P. Funk. Über Flächen mit lauter geschlossenen geodätischen Linien. *Math. Ann.*, 74(2):278 – 300, 1913.
12. S. Gindikin, J. Reeds, and L. Shepp. Spherical tomography and spherical integral geometry. In E. T. Quinto, M. Cheney, and P. Kuchment, editors, *Tomography, Impedance Imaging, and Integral Geometry*, volume 30 of *Lectures in Appl. Math*, pages 83–92. American Mathematical Society, South Hadley, Massachusetts, 1994.
13. P. Goodey and W. Weil. Average section functions for star-shaped sets. *Adv. in Appl. Math.*, 36(1):70–84, 2006.
14. I. S. Gradshteyn and I. M. Ryzhik. *Table of Integrals, Series, and Products*. Academic Press New York, seventh edition, 2007.
15. M. Gräf. Quadrature rules on manifolds. `http://www.tu-chemnitz.de/~potts/workgroup/graef/quadrature`.
16. M. Gräf. *Efficient Algorithms for the Computation of Optimal Quadrature Points on Riemannian Manifolds*. Dissertation. Universitätsverlag Chemnitz, 2013.
17. M. Gräf and D. Potts. Sampling sets and quadrature formulae on the rotation group. *Numer. Funct. Anal. Optim.*, 30:665–688, 2009.
18. H. Groemer. On a spherical integral transformation and sections of star bodies. *Monatsh. Math.*, 126(2):117–124, 1998.

19. D. M. Healy, Jr., H. Hendriks, and P. T. Kim. Spherical deconvolution. *J. Multivariate Anal.*, 67:1–22, 1998.
20. S. Helgason. *Integral Geometry and Radon Transforms*. Springer, 2011.
21. R. Hielscher. The Radon Transform on the Rotation Group–Inversion and Application to Texture Analysis. Dissertation, Technische Universität Bergakademie Freiberg, 2007.
22. R. Hielscher and M. Quellmalz. Optimal mollifiers for spherical deconvolution. *Inverse Problems*, 31(8):085001, 2015.
23. R. Hielscher and M. Quellmalz. Reconstructing a function on the sphere from its means along vertical slices. *Inverse Probl. Imaging*, 10(3):711 – 739, 2016.
24. J. Keiner, S. Kunis, and D. Potts. NFFT 3.3, C subroutine library. `http://www.tu-chemnitz.de/~potts/nfft`.
25. J. Keiner, S. Kunis, and D. Potts. Efficient reconstruction of functions on the sphere from scattered data. *J. Fourier Anal. Appl.*, 13:435–458, 2007.
26. J. Keiner and D. Potts. Fast evaluation of quadrature formulae on the sphere. *Math. Comput.*, 77:397–419, 2008.
27. A. K. Louis and P. Maass. A mollifier method for linear operator equations of the first kind. *Inverse Problems*, 6(3):427–440, 1990.
28. V. Michel. *Lectures on Constructive Approximation: Fourier, Spline, and Wavelet Methods on the Real Line, the Sphere, and the Ball*. Birkhäuser, New York, 2013.
29. G. Nolet. *A Breviary of Seismic Tomography*. Cambridge University Press, Cambridge, 2008.
30. V. P. Palamodov. *Reconstruction from Integral Data*. Monographs and Research Notes in Mathematics. CRC Press, Boca Raton, 2016.
31. V. P. Palamodov. Reconstruction from cone integral transforms. *Inverse Problems*, 33(10):104001, 2017.
32. D. Potts, J. Prestin, and A. Vollrath. A fast algorithm for nonequispaced Fourier transforms on the rotation group. *Numer. Algorithms*, 52:355–384, 2009.
33. M. Quellmalz. A generalization of the Funk–Radon transform. *Inverse Problems*, 33(3):035016, 2017.
34. B. Rubin. Generalized Minkowski-Funk transforms and small denominators on the sphere. *Fract. Calc. Appl. Anal.*, 3(2):177–203, 2000.
35. B. Rubin. Radon transforms and Gegenbauer-Chebyshev integrals, II; examples. *Anal. Math. Phys.*, Advance online publication, 2016.
36. B. Rubin. On the determination of star bodies from their half-sections. *Mathematika*, 63(2):462–468, 2017.
37. Y. Salman. An inversion formula for the spherical transform in S^2 for a special family of circles of integration. *Anal. Math. Phys.*, 6(1):43 – 58, 2016.
38. R. Schneider. Functions on a sphere with vanishing integrals over certain subspheres. *J. Math. Anal. Appl.*, 26:381–384, 1969.
39. R. S. Strichartz. L^p estimates for Radon transforms in Euclidean and non-Euclidean spaces. *Duke Math. J.*, 48(4):699–727, 1981.
40. J. Trampert and J. H. Woodhouse. Global phase velocity maps of love and rayleigh waves between 40 and 150 seconds. *Geophys. J. Int.*, 122(2):675–690, 1995.
41. D. Varshalovich, A. Moskalev, and V. Khersonskii. *Quantum Theory of Angular Momentum*. World Scientific Publishing, Singapore, 1988.
42. E. Wigner. *Gruppentheorie und ihre Anwendung auf die Quantenmechanik der Atomspektren*, volume 85 of *Die Wissenschaft*. Friedr. Vieweg & Sohn, 1931.
43. J. H. Woodhouse and A. M. Dziewonski. Mapping the upper mantle: Three-dimensional modeling of earth structure by inversion of seismic waveforms. *J. Geophys. Res. Solid Earth*, 89(B7):5953–5986, 1984.
44. G. Zangerl and O. Scherzer. Exact reconstruction in photoacoustic tomography with circular integrating detectors II: Spherical geometry. *Math. Methods Appl. Sci.*, 33(15):1771–1782, 2010.